Frustration-induced quantum criticality in Ni-doped CePdAl as revealed by the μSR technique

I. Ishant, T. Shiroka, O. Stockert, Veronika Fritsch, M. Majumder

Angaben zur Veröffentlichung / Publication details:

Ishant, I., T. Shiroka, O. Stockert, Veronika Fritsch, and M. Majumder. 2024. "Frustration-induced quantum criticality in Ni-doped CePdAl as revealed by the μSR technique." *Physical Review Research* 6 (2): 023112. https://doi.org/10.1103/physrevresearch.6.023112.

Frustration-induced quantum criticality in Ni-doped CePdAl as revealed by the μSR technique

I. Ishant [1], T. Shiroka [2,3,*], O. Stockert [4], V. Fritsch [5], and M. Majumder [1,†]

[1] Department of Physics, Shiv Nadar Institution of Eminence, Gautam Buddha Nagar, Uttar Pradesh 201314, India
[2] Laboratory for Muon-Spin Spectroscopy, Paul Scherrer Institut, CH-5232 Villigen PSI, Switzerland
[3] Laboratorium für Festkörperphysik, ETH Zürich, CH-8093 Zürich, Switzerland
[4] Max Planck Institute for Chemical Physics of Solids, 01187 Dresden, Germany
[5] Experimental Physics VI, Center for Electronic Correlations and Magnetism, University of Augsburg, 86159 Augsburg, Germany

(Received 13 December 2023; revised 22 February 2024; accepted 27 March 2024; published 1 May 2024)

In CePdAl, the $4f$ moments of cerium arrange to form a geometrically frustrated kagome lattice. Due to frustration, in addition to Kondo and Ruderman-Kittel-Kasuya-Yosida interactions, this metallic system shows a long-range magnetic order (LRO) with a T_N of only 2.7 K. Upon Ni doping at the Pd sites, T_N is further suppressed, to reach zero at a critical concentration $x_c \approx 0.15$. Here, by using muon-spin relaxation and rotation (μSR), we investigate $CePd_{1-x}Ni_xAl$ at a local level for five different Ni concentrations, both above and below x_c. Like the parent CePdAl compound, for $x = 0.05$, we observe an incommensurate LRO, which turns into a quasistatic magnetic order for $x = 0.1$ and 0.14. More interestingly, away from x_c, for $x = 0.16$ and 0.18, we still observe a non-Fermi-liquid (NFL) regime, evidenced by a power-law divergence of the longitudinal relaxation at low temperatures. In this case, longitudinal field measurements exhibit a time-field scaling, indicative of cooperative spin dynamics that persists for $x > x_c$. Furthermore, like the externally applied pressure, the chemical pressure induced by Ni doping suppresses the region below T^*, characterized by a spin-liquid-like dynamical behavior. Our results suggest that the magnetic properties of CePdAl are similarly affected by the hydrostatic and the chemical pressure. We also confirm that the unusual NFL regime (compared with conventional quantum critical systems) is due to the presence of frustration that persists up to the highest Ni concentrations.

DOI: 10.1103/PhysRevResearch.6.023112

I. INTRODUCTION

Heavy-fermion compounds with partially localized d- or f-magnetic moments have long been at the center of numerous theoretical and experimental studies [1]. The interest in these strongly correlated electron systems stems from the plethora of phenomena they exhibit, such as quantum criticality [2,3], hidden order [4], charge-density wave [5], or the possibility to behave as superconductors [6], topological insulators [7], or topological Weyl semimetals [8,9]. In magnetic heavy-fermion compounds, two types of interactions dominate. One of them is the Ruderman-Kittel-Kasuya-Yosida (RKKY) interaction, where the conduction electrons mediate the interaction between the local magnetic moments which, consequently, tend to form a long-range order (LRO). If the coupling between the local moments and the conduction electrons is J, the strength of the RKKY interaction varies as $T_{RKKY} \propto J^2$ [10,11]. On the other hand, the Kondo interaction arises because of the formation of many-body singlet states between the local moments and the conduction electrons. Since it screens the local moments, it tends to suppress the magnetic ordering temperature. The strength of the Kondo interaction varies as $T_K \propto e^{(-1/J)}$ [12]. In the 1970s, Doniach [13] proposed a phase diagram which reflects the J dependence of the two interactions and indicates that, for small values of J, the RKKY interaction dominates, while for high values of J, the Kondo interaction dominates. Because of the competition between these two interactions, at a particular value of J, the LRO disappears. Thus, by utilizing a nonthermal tuning parameter (such as pressure, magnetic field, or doping), one can tune J and continuously suppress the second-order phase transition to $T = 0$, to reach the so-called quantum critical point (QCP). Quantum fluctuations at the QCP break down the Fermi-liquid model, and a non-Fermi-liquid (NFL) behavior [14,15] is expected to show up in different physical properties, such as magnetic susceptibility, heat capacity, and spin-lattice relaxation rate.

Recently, a global phase diagram has been proposed on top of the Kondo and RKKY interactions [16], incorporating the effects of quantum fluctuations (which increase with increasing frustration). The inclusion of frustration, arising from local moments arranged into a triangular, kagome, Shastry-Sutherland, or pyrochlore lattice, induces different types of quantum criticality (local and spin-density wave type) [17,18] and exotic phases of matter, e.g., quantum-spin liquids (QSLs) [19]. A QSL is an entangled state where magnetic moments, despite being highly correlated, do not break any symmetry, even down to $T = 0$. Unlike in insulators, where QSL states are more common, in metallic systems, they are quite

*toni.shiroka@psi.ch
†mayukh.cu@gmail.com

rare. However, in some frustrated metallic systems, such as CeRhSn [20], $Pr_2Ir_2O_7$ [21], $CeRh_{1-x}Pd_xSn$ [22], and CeIrSn [23], QSL-type spin dynamics has been observed. Metallic systems with magnetic moments lying in a frustrated lattice are comparatively less explored, but nonetheless intriguing. For instance, in the absence of Dzyaloshinskii-Moriya interactions, skyrmion spin textures have been observed in $4f$-based metallic systems with a frustrated lattice [24,25].

In this respect, CePdAl, where the Ce moments are arranged in a highly frustrated kagome lattice [26], is a very promising system for exploring the above mentioned topics. CePdAl (with $T_N \approx 2.7$ K) is also very susceptible to tuning. Thus, hydrostatic pressure can suppress the LRO, and a QCP emerges at a P_c of ∼0.9 GPa. More interestingly, an extended NFL regime with QSL-like dynamic correlations has been observed up to about twice P_c. Such a phase was claimed to be due to the presence of frustration [27,28]. Thus, the presence of frustration not only stabilizes the QSL state, but it also changes the generic features of the QCP by producing an extended NFL regime well beyond the critical point. As the lattice parameters were found to decrease with increasing Ni doping [26], the resulting chemical pressure caused by Ni replacement at the Pd sites suppresses T_N to 0 K at a critical concentration $x_c \approx 0.15$. In this case, the relevant questions are: What is the nature of the critical fluctuations around QCP? Is there any extended NFL regime/state also with chemical pressure? What are the similarities or dissimilarities between the hydrostatic and chemical pressure? Is frustration responsible for the NFL behavior, or can the (chemical-doping induced) disorder account for it? To answer these questions, we employed a well-known local-probe technique, muon-spin relaxation/rotation (μSR). All samples were specimens of Czochralski-grown single crystals which were powderized and pressed into pellets for the measurements. The μSR experiments were performed on $CePd_{1-x}Ni_xAl$ with five different Ni concentrations x, both above and below $x_c = 0.15$: 0.05, 0.1, 0.14, 0.16, and 0.18 on the Dolly spectrometer of the Swiss Muon Source (SμS) at the Paul Scherrer Institute, Switzerland. The base temperature for the Dolly spectrometer is 270 mK, reached by using a ^{3}He cryostat. Such an extensive investigation allowed us not only to answer the above questions, but also to construct a comprehensive phase diagram of CePdAl under Ni doping.

II. EXPERIMENTAL RESULTS

The NFL behavior in a metal arises from its low-lying quasi-particle excitations, to which a low-frequency probe like μSR is quite sensitive. Thus, extensive (μSR) measurements were performed to elucidate the complex phase diagram of $CePd_{1-x}Ni_xAl$. The details of the different μSR experiments, along with the results obtained, are discussed in the following sections.

A. Weak transverse field measurements

Weak transverse field (wTF) measurements allow us to extract the temperature dependence of the nonmagnetic volume fraction from which the magnetic ordering temperature can be estimated. The terms weak and transverse indicate that the applied field is less than the internal field (and low enough so that it does not deviate the muon beam) and that the applied magnetic field is transverse with respect to the direction of the muon spin, respectively. The wTF spectra were collected in a 3-mT applied field at several temperatures and in samples with different Ni concentrations. Figure 1(a) depicts the wTF asymmetry of the $x = 0.1$ sample at 0.27 and 10 K. The wTF asymmetries were fitted by a combination of an exponentially relaxing oscillatory component, representing the paramagnetic spins, and a fast exponentially relaxing nonoscillatory component, representing the spins taking part in the magnetic ordering [solid lines in Fig. 1(a)]:

$$A(t) = A_0[f_{pm}\cos(\omega t + \phi_{TF})\exp(-\lambda_{pm}t) + (1 - f_{pm})\exp(-\lambda_{ord}t)]. \quad (1)$$

Here, $A(t)$ is the time-dependent muon asymmetry, with A_0 the initial asymmetry. Further, f_{pm}, ω, ϕ_{TF}, and λ_{pm} are the fraction of spins, the muon Larmor frequency, the initial phase, and the relaxation rate in the paramagnetic state. Finally, λ_{ord} is the relaxation rate in the magnetically ordered

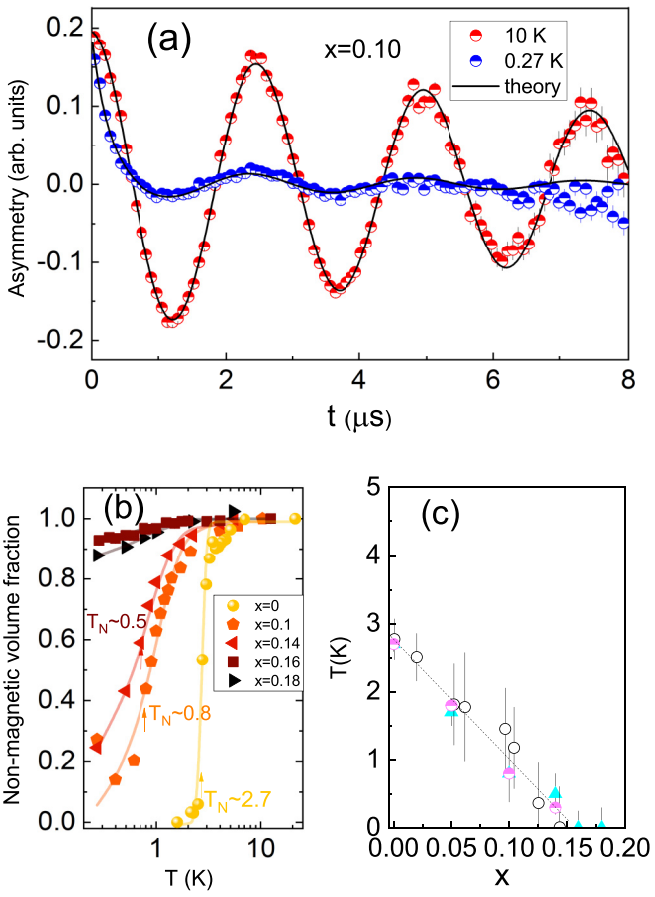

FIG. 1. (a) Weak transverse field (wTF)-μSR asymmetry of $x = 0.1$ in a 3 mT applied field. (b) Nonmagnetic volume fraction vs. temperature estimated from wTF measurements for different Ni concentrations. Solid lines are fits using Eq. (2). (c) Temperature-concentration diagram of Ni-doped CePdAl resulting from wTF-μSR data. The dotted line is a linear fit. Triangles represent T_N from this paper, while heat-capacity data (open circles) and neutron-scattering results (half-filled circles) are taken from Refs. [26,29], respectively.

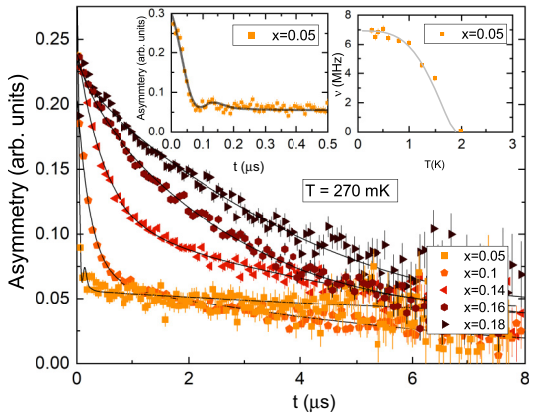

FIG. 2. Zero-field μSR asymmetry for different Ni concentrations. Solid lines are fits to the equations described in the text. Insets show the short-time μSR asymmetry (left) and ν vs temperature (right) for the $x = 0.05$ case.

phase. At the highest temperature, the externally applied field dominates the internal field ($H_{\rm ext} \gg H_{\rm int}$), thus giving rise to asymmetry oscillations with the highest $f_{\rm pm}$, indicative of a fully paramagnetic state. As T decreases, the oscillation amplitude $f_{\rm pm}$ decreases, indicating the onset of a spontaneous internal field. At the same time, $(1 - f_{\rm pm})$ increases as the temperature decreases, indicating the enhanced magnetic contribution related to the LRO. As shown in Fig. 1(b), the temperature dependence of $f_{\rm pm}$ (the nonmagnetic volume fraction) was fitted with an empirical sigmoidal function:

$$A(T) = A_a + \frac{A_b - A_a}{1 + \exp\left(\frac{T - T_{\rm N}}{\Delta T}\right)}. \tag{2}$$

Here, $T_{\rm N}$ is the ordering temperature, and ΔT is the transition width. Also, A_a and A_b are the asymmetries above and below $T_{\rm N}$, respectively. The suppression of $T_{\rm N}$ of CePdAl as the Ni doping increases is shown in Fig. 1(c). Our results are consistent with those from magnetization and heat-capacity measurements [26,29]. The linear suppression of $T_{\rm N}$ with Ni doping yields a critical concentration $x_c \approx 0.15$.

B. Zero-field measurements

Zero-field (ZF) μSR measurements are sensitive to small magnetic moments (as small as 0.001 $\mu_{\rm B}$) and, thus, are a powerful tool to study weak internal fields and a possible magnetic order. The time dependence of ZF- μSR asymmetry provides useful hints into the nature of the LRO state and the quantum critical behavior of the electron spin dynamics close to the QCP.

1. Magnetically ordered state (for $x < x_c$)

Figure 2 shows the ZF-μSR asymmetry spectra of all the samples ($x = 0.05$, 0.1, 0.14, 0.16, and 0.18), recorded at 0.27 K. For $x = 0.05$, the ZF-μSR asymmetry is very similar to that of the CePdAl parent compound. In this case, the same function used for CePdAl [27] provides perfect fits:

$$A(t) = A_0\left\{f_{\rm sample}\left[\frac{2}{3}j_0(2\pi\nu t + \phi)\exp\left(\frac{-\sigma^2 t^2}{2}\right) + \frac{1}{3}\exp(\lambda_L t)\right] + (1 - f_{\rm sample})\exp(-\lambda_{\rm bkg} t)\right\}. \tag{3}$$

Here, A_0 is the initial asymmetry, and σ is the depolarization rate caused by the distribution of internal fields, ν is the frequency of the oscillating component, and ϕ is its phase (here, kept at zero). Furthermore, λ_L is the longitudinal relaxation rate, $f_{\rm sample}$ is the fraction of moments involved in the LRO, and $\lambda_{\rm bkg}$ is the background relaxation contribution. As shown in the inset of Fig. 2, below $T_{\rm N}$, the order parameter can be mapped into the oscillation frequency, whose temperature dependence for the $x = 0.05$ case is described by $\nu(T) = \nu_0[1 - (T/T_{\rm N})^{\delta}]^{\eta}$, with $\delta = 3.5$ and $\eta = 2$. Here, ν_0 is the local field at the muon site, extrapolated to $T = 0$. This is shown to vary linearly with the ordering temperature $T_{\rm N}$ (see inset in Fig. 6), here, an implicit function of pressure [27]. Here, $T_{\rm N}$ is shown to correlate linearly also with the ordered magnetic moment (estimated from neutron diffraction experiments [29]), thus strongly suggesting that, as expected, the local magnetic field at the muon stopping site is proportional to the ordered moment.

Interestingly, at higher Ni doping ($x = 0.1$ and 0.14), no spontaneous muon spin precession is observed down to 0.27 K, despite a magnetic ordering taking place at 0.8 and 0.5 K, respectively (as determined from wTF-μSR data). Below these ordering temperatures, the ZF-μSR asymmetry of the $x = 0.1$ and 0.14 samples is well fitted by the sum of two exponential functions, one with a slow and one with a fast relaxation rate:

$$A(t) = A_0\{f_s[\exp(-\lambda_s T)] + f_f[\exp(-\lambda_f T)]\}. \tag{4}$$

Here, A_0 is the initial asymmetry, fixed at the highest temperature, f_s and f_f ($= 1 - f_s$) are the fractions of the slow and the fast relaxation components, while λ_s and λ_f are the respective muon-spin relaxation rates. The temperature dependences of λ_f, λ_s, and f_f are shown in Fig. 3. As the temperature

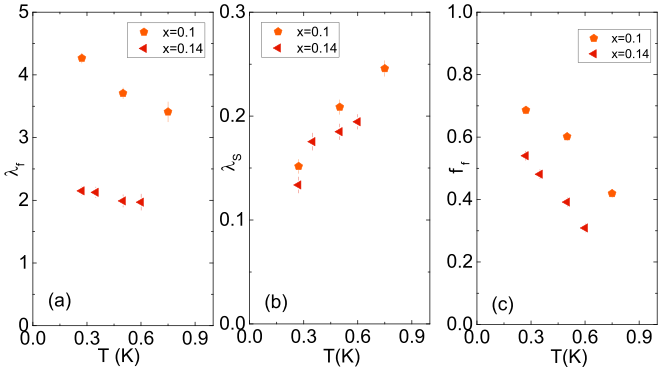

FIG. 3. Temperature dependence of (a) λ_f, (b) λ_s, and (c) f_f for $x = 0.1$ and 0.14.

is lowered, λ_f and f_f increase, while λ_s decreases. Since the f_f fraction increases to $\sim$0.66 ($\sim\frac{2}{3}$) and λ_f shows an order-parameter-like behavior, we identify the fast and slow components with the transverse and longitudinal relaxation, respectively. Their behavior can be ascribed either to a quasistatic magnetic ordering, as also found in other disordered systems, or to an incommensurate ordering, the later leading to a broad distribution of local magnetic fields at the muon stopping site [30,31]. The incommensurate ordering, however, may be discarded for the present systems, as we observe clear oscillations in the asymmetry due to incommensurate ordering at ambient and applied pressure [27], which indicates that the local magnetic field distribution here is not broad enough to completely wipe out the oscillation. On the other hand, disorder originating from Ni doping is a more likely explanation for the evolution of the LRO (in $x = 0.05$) into a quasistatic magnetic order at higher Ni concentrations (see Fig. 6). The role of disorder is confirmed also by the increased broadening of the magnetic Bragg peak at $Q_{\rm AF}$ (0.5, 0, 0.35) with increasing Ni content [29], a result at least partially attributed to disorder, which further corroborates our hypothesis. Note that we attempted to fit the ZF-μSR asymmetry with various functions relevant for different types of disordered states, e.g., spin glass (SG) [32], inhomogeneous magnetic moments with short-range correlations [33–36], and quantum Griffiths states [37]. Since none of them fit the data adequately, we conclude that the degree of disorder in $CePd_{1-x}Ni_xAl$ is rather small compared with those states. In the Discussion section, we elaborate in more detail about the role of disorder.

2. Paramagnetic state

In the paramagnetic state, the ZF-μSR asymmetry can be well fitted by a static Gaussian Kubo-Toyabe function, representing the nuclear moment contribution, multiplied by a stretched exponential function, representing the contribution of the electronic moments:

$$A(t) = A_0\left\{\frac{1}{3} + \frac{2}{3}\left(1-\sigma_{\rm n}^2 t^2\right)\exp\left[-\left(\frac{\sigma_{\rm n}^2 t^2}{2}\right)\right] \times \exp[-(\lambda t)^{\beta}]\right\}. \quad (5)$$

Here, λ and $\sigma_{\rm n}$ are the exponential and Gaussian relaxation rates, the latter found to be temperature independent, with $\sigma_{\rm n} = 0.13\,\mu{\rm s}^{-1}$. Conversely, both λ and β depend on temperature. At high temperatures, the value of β is 1, representing a fixed-field distribution and simple random rapid fluctuations. Upon lowering the temperature, β decreases from 1, and λ increases. In Fig. 4(a), we show the temperature dependence of the relaxation rate $\lambda/T = 1/T_{1\mu}T \propto \chi''(q,\omega)$, where $\chi''(q,\omega)$ is the imaginary part of the dynamical spin susceptibility. For $x = 0.05$, 0.1, and 0.14, λ/T diverges toward $T_{\rm N}$ due to the critical slowing down of spin fluctuations by following a power-law $T^{-\alpha}$, whose exponent α decreases with increasing Ni concentration.

More interestingly, above the critical $x_c \approx 0.15$ value (for $x = 0.16$ and 0.18), the power-law behavior of λ/T still persists. Such an extension of the NFL regime above the critical value of the tuning parameter (here, x_c) has also been seen in pressurized CePdAl, indicating the same effect of chemical and hydrostatic pressure on CePdAl.

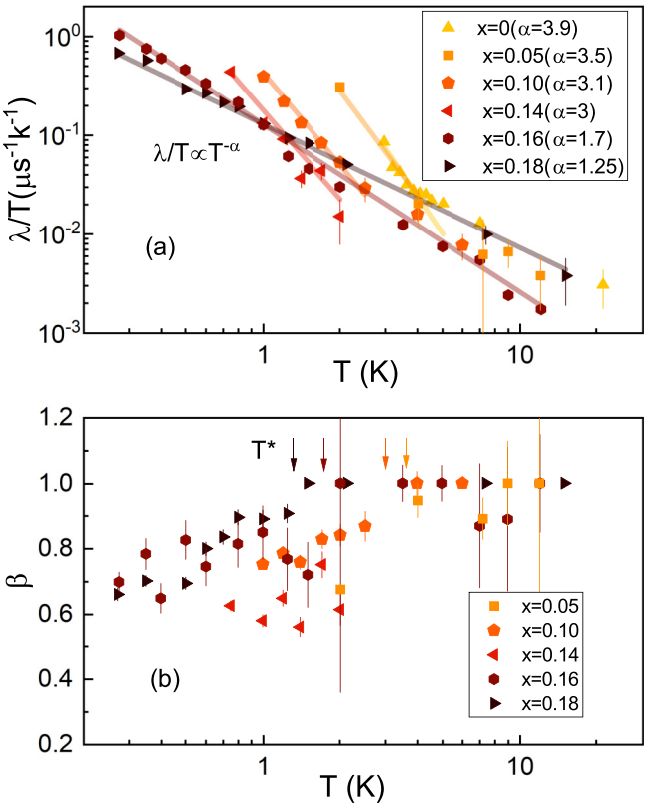

FIG. 4. (a) Temperature dependence of the λ/T for all the Ni concentrations. Solid lines represent power-law fits, $T^{-\alpha}$. (b) Stretching exponent β for various Ni concentrations as a function of temperature. Arrows indicate the onset of the spin-liquid regime at T^*.

C. Longitudinal field measurements

μSR measurements in a longitudinal field (LF) allowed us to determine the nature of the electron-spin dynamics close to the QCP. Figure 5(a) shows the LF dependence of λ at 0.27 K for $x = 0.16$ and 0.18 (i.e., both above x_c). The main cause of the muon-spin relaxation is usually the spin fluctuations of $4f$ electrons, whose magnetic moments couple with those of the implanted muons. To have a quantitative idea about the nature of spin dynamics at low temperature, we utilized the following function [38–40]:

$$\lambda(H) = 2\Delta^2\tau^{x'}\int_0^{\infty} t^{-x'}e^{-\nu t}\cos(2\pi\mu_0\gamma_\mu H t)\,dt, \quad (6)$$

where t is time, τ is an early-time cutoff, Δ is the width of the internal-field distribution, γ_μ is the gyromagnetic ratio, and ν is the fluctuation frequency of local moments. A fit of the LF dependence of λ [see Fig. 5(a)] yields $x' \neq 0$, which indicates that the spin-spin autocorrelation function is not a simple exponential $C(t) = \exp(-\nu t)$, but rather $C(t) = (\tau/t)^{x'}\exp(-\nu t)$. The fluctuation frequency ν, for $x = 0.16$ and 0.18, is estimated to be 315 and 172 MHz, respectively. In either case, ν is two orders of magnitude higher than commonly found in other spin-liquid candidate

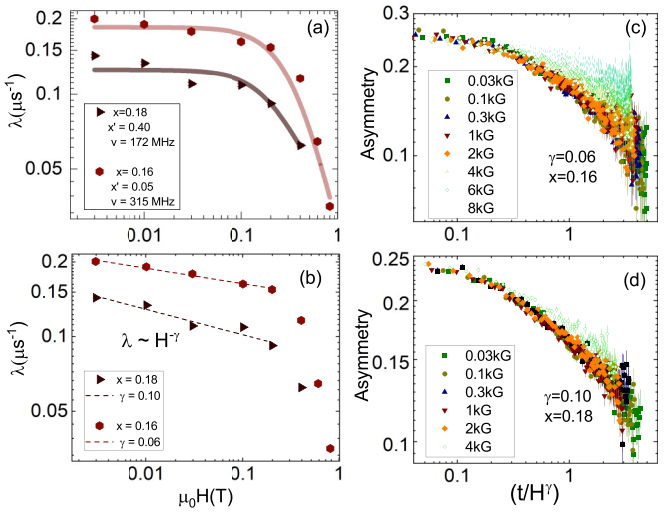

FIG. 5. (a) and (b) μSR relaxation rate λ vs longitudinal field for $x = 0.14$, 0.16, and 0.18. (a) Solid lines represent fits using Eq. (6), while (b) dashed lines are power-law fits, $\lambda \propto H^{-\gamma}$. Time-field scaling of the μSR asymmetry at 0.27 K for (c) $x = 0.16$ and (d) $x = 0.18$.

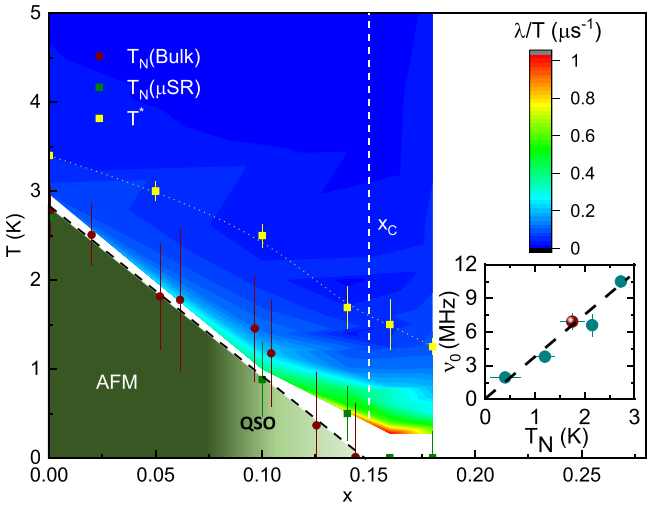

FIG. 6. Temperature-concentration magnetic phase diagram of Ni-doped CePdAl combined with a contour plot of the concentration and temperature-dependent relaxation rate $\lambda/T(x, T)$. The Néel temperatures T_N estimated from wTF-μSR (green squares, with error bars indicating the width of transition) agree well with the reported values from susceptibility measurements (filled circles). Yellow squares represent $T^*(x)$. QSO stands for quasistatic magnetic ordering, as discussed in the text. Inset shows ν_0 vs ordering temperature T_N (the dashed line is a linear fit). The brown and the cyan circles correspond to the doping and pressure evolution of T_N and ν_0, respectively.

materials $NaYbS_2$ [41], $YbMgGaO_4$ [39], $Sr_3CuSb_2O_9$ [42], and $BaTi_{0.5}Mn_{0.5}O_3$ [40] but of similar order of magnitude to other metallic heavy-fermion compounds close to quantum criticality [43,44]. However, the present ν values are slower than those of many SG materials [45].

Interestingly, for applied magnetic fields $\mu_0 H$ between 3 and 200 mT, we also identify a time-field scaling $A(t/H^\gamma)$, where γ is an exponent. Such field dependence corresponds to evaluating the Fourier transform of $C(t) = \langle \mathbf{S}_i(0) \cdot \mathbf{S}_i(t) \rangle$ throughout the 0.4 to 28 MHz frequency range ($\gamma_\mu H/2\pi$). Time-field scaling is a signature of slow dynamics that is encountered in both classical SGs and in NFL systems with local $4f$ moments. Independent information on the behavior of the spin-spin autocorrelation function $C(t)$ may be gained by examining the time-field scaling. While $\gamma < 1$ signifies a power-law behavior of $C(t)$, $\gamma > 1$ implies a stretched exponential behavior, typical of inhomogeneous systems. In Figs. 5(c) and 5(d), we show the asymmetry vs the time-scaling variable $A(t/H^\gamma)$, for $x = 0.16$ and 0.18, respectively. Since in both cases we find an exponent $\gamma < 1$, this indicates a power-law behavior of $C(t)$, consistent with an analysis by means of Eq. (6). The exponent γ also matches the power-law exponent in the λ vs applied field plot shown in Fig. 5(b) up to 0.2 T. A similar time-field scaling has been found in $UCu_{5-x}Pd_x$ [46], $CePtSi_{1-x}Ge_x$ [47], and $CePd_{0.15}Rh_{0.85}$ [48]. The high-field data (here, >0.2 T) deviate from the scaling curve as well as from the power-law behavior [Fig. 5(b)], indicating that higher applied fields have a direct effect on $C(t)$. A similar kind of deviation has also been seen in $Ce(Cu_{1-x}Co_x)_2Ge_2$ [49]. Our LF experiments strongly suggest a cooperative spin dynamics in the spin-liquid regime above x_c and below T^*. Furthermore, the LF experiments also indicate that even a field of 0.8 T is not enough to completely suppress the relaxation process and suggest that the correlations are dynamic in nature, as can be expected in the QSL state.

III. DISCUSSION

Our pressure-temperature phase diagram [27] shows that the extended NFL regime is exclusively due to frustration, as pressure does not introduce significant disorder. Since chemical doping may introduce disorder and an extended NFL regime also occurs in several disordered heavy-fermion compounds [50,51], it is important to clarify whether disorder or frustration is responsible for the magnetic properties of $CePd_{1-x}Ni_xAl$ above x_c.

A. Effect of disorder

Disorder-induced states include the quantum Griffiths phase (QGP) and SGs. The QGP appears in systems where the quenched disorder radically affects a quantum-phase transition giving rise to an additional QGP phase. In such a case, a smeared phase transition can occur near the QCP. In $CePd_{1-x}Ni_xAl$, however, this smearing effect is not observed (at least not down to 0.27 K), which is low enough with respect to the temperatures below which QGPs have been found in other systems [37,49,52]. Thus, we can discard the possibility of such a phase. It should be noted that λ/T obeys a power-law $T^{-\alpha}$ behavior, with $\alpha > 1$ in the $CePd_{1-x}Ni_xAl$ case. In other QGP systems, however, the power-law exponent is found to be <1, e.g., in $Ce(Cu_{1-x}Co_x)_2Ge_2$ ($\alpha = 0.55$) [49], in $CeCoGe_{3-x}Si_x$ ($\alpha = 0.72$) [53], and in $CePd_{0.15}Rh_{0.85}$ ($\alpha = 0.8$) [48]. This indicates that disorder suppresses the critical fluctuations.

Now we consider the possibility of a SG state occurring in $CePd_{1-x}Ni_xAl$. The absence of spin freezing in Ni-doped

CePdAl is supported by the following observations: (i) SG is also a disordered magnetic state, where spins are statically aligned randomly, so that the dynamics is very slow, usually between 0.01 and 0.1 ns [45]. Our LF-μSR measurements indicate a time scale of ∼3–5 ns, more than an order of magnitude larger than that of SG systems (mentioned in the previous section). (ii) The stretching exponent β decreases gradually from 1 at high temperatures to a constant value of 0.6 at low temperatures [see Fig. 4(b)]. On the other hand, for SG systems, β is expected to decrease to $\frac{1}{3}$ at the spin freezing temperature [54,55]. (iii) As already discussed in the previous section, we were unable to fit the μSR asymmetry by considering any function relevant for the SG state.

At the same time, resistivity measurements at higher Ni doping [56] show a negligible distribution of Kondo temperatures. This further indicates that Ni doping introduces at most only a weak disorder. Thus, it can be stated that the weak disorder introduced by Ni doping is unable to form either QGP or SG states in $CePd_{1-x}Ni_xAl$. The quasistatic state observed for $x = 0.1$ and 0.14 may be an unconventional, weak disorder-induced state. Along with the above mentioned points, the incompatibility of fitting the asymmetry with different fit functions used for various disordered states supports the absence of strong disorder effects.

Usually, the lower the value of the exponent γ, the lesser the chance of having a disordered ground state. Thus, in the present case, $\gamma \ll 1$ (discussed in the previous section) excludes a dominant effect of disorder in the critical fluctuations around the QCP. Since the effect of chemical and hydrostatic pressure on CePdAl is identical (as far as the magnitude of λ/T and the power-law exponents are concerned), this again supports the weak effect of disorder in determining the NFL regime in this compound.

B. Effect of frustration

It is interesting to note that, for $x = 0$, 0.05, and 0.1, the enhancement of λ/T [see Fig. 4(a)] starts from a temperature tenfold above T_N, indicating a high degree of frustration in $CePd_{1-x}Ni_xAl$. Neutron scattering also detects short-range correlations at a temperature much higher than T_N. Also for $x = 0.16$ and 0.18, the enhancement of λ/T from a very high temperature suggests the significant role of frustration on the quantum critical nature of spin fluctuations. Note that such an enhancement of λ/T from a very high temperature was not observed in other Ce-based systems [22,48,49] lacking a geometrically frustrated lattice. This implies that frustration persists throughout the full doping range studied in this paper, and it provides evidence that frustration is responsible for the extended NFL regime (at $x > x_c$) in CePdAl.

The presence of finite frustration is also reflected in the temperature dependence of β shown in Fig. 4(b). Our pressure-dependent μSR study identifies a characteristic temperature T^*, below which β deviates from 1. This was assigned to the temperature below which spin-liquid-like correlations develop [27]. In the present case, too, such a characteristic temperature T^* exists and is found to decrease with increasing Ni concentration, as shown in Fig. 4(b). This again confirms the similarity between the hydrostatic and chemical pressure effects in the magnetic properties of CePdAl. These observations indicate the importance of frustration on the quantum critical fluctuations and also the persistence of frustration throughout the full doping range.

From the above discussion, we have established that disorder has only a limited role in originating the NFL regime in $CePd_{1-x}Ni_xAl$, while the persistent frustration is clearly responsible for the extended NFL regime. The weak disorder seems to affect and stabilize only the quasistatic ordered state for $x < x_c$.

IV. CONCLUSIONS

In conclusion, by utilizing the local-probe μSR technique, we investigated the quantum critical Ni-doped CePdAl system across the full range of Ni concentrations, both above and below $x_c = 0.15$. For $x = 0.05$, we observe an incommensurate LRO state, like that of the CePdAl parent compound. Upon increasing the Ni concentration, disorder appears, and the LRO changes into a quasistatic magnetic order for $x = 0.1$ and 0.14. This state does not exhibit the properties expected for a conventional SG or quantum Griffiths state, thus indicating a relatively low amount of Ni-induced disorder in this system. Interestingly, a power-law dependence of the longitudinal relaxation rate and a time-field scaling are observed for $x = 0.16$ and 0.18, suggesting a NFL regime. Since both values lie above x_c, our results indicate that the NFL regime extends beyond x_c, thus mimicking the behavior of the pressure-induced phase diagram of CePdAl. Since frustration is shown to persist up to $x = 0.18$, the extended NFL regime is, therefore, due to frustration. Akin to the pressure effect on the magnetic properties of pure CePdAl, the chemical pressure in the Ni-doped case also reduces a characteristic temperature T^*, below which spin-liquid-like dynamical fluctuations occur in the $x = 0.16$ and 0.18 case. In summary, all our observations suggest a similar role for the hydrostatic and chemical pressure on the magnetic properties of CePdAl, with frustration being the main driving force behind such unusual behavior. In the future, it might be interesting to see how far (in terms of Ni doping) such a frustration-driven NFL regime persists until the Fermi liquid emerges.

ACKNOWLEDGMENTS

This work is based on experiments performed at the Swiss Muon Source SμS, Paul Scherrer Institute, Villigen, Switzerland.

V.F. and O.S. prepared the sample and initiated the study of CePdAl. T.S. performed the μSR measurements, with the online assistance of I.I and M.M.. I.I and M.M. analyzed the data. I.I.,M.M., and T.S. wrote the manuscript with notable inputs from all the coauthors. M.M. supervised the project.

[1] Q. Si, S. Rabello, K. Ingersent, and J. L. Smith, Locally critical quantum phase transitions in strongly correlated metals, Nature (London) **413**, 804 (2001).

[2] M. Brando, D. Belitz, F. M. Grosche, and T. R. Kirkpatrick, Metallic quantum ferromagnets, Rev. Mod. Phys. **88**, 025006 (2016).

[3] P. Coleman and A. J. Schofield, Quantum criticality, Nature (London) **433**, 226 (2005).

[4] T. T. M. Palstra, A. A. Menovsky, J. van den Berg, A. J. Dirkmaat, P. H. Kes, G. J. Nieuwenhuys, and J. A. Mydosh, Superconducting and magnetic transitions in the heavy-fermion system URu_2Si_2, Phys. Rev. Lett. **55**, 2727 (1985).

[5] Z. Hossain, M. Schmidt, W. Schnelle, H. S. Jeevan, C. Geibel, S. Ramakrishnan, J. A. Mydosh, and Y. Grin, Coexistence of magnetic order and charge density wave in a Kondo lattice: $Yb_5Ir_4Si_{10}$, Phys. Rev. B **71**, 060406(R) (2005).

[6] F. Steglich, J. Aarts, C. D. Bredl, W. Lieke, D. Meschede, W. Franz, and H. Schäfer, Superconductivity in the presence of strong Pauli paramagnetism: $CeCu_2Si_2$, Phys. Rev. Lett. **43**, 1892 (1979).

[7] J. Jiang, S. Li, T. Zhang, Z. Sun, F. Chen, Z. R. Ye, M. Xu, Q. Q. Ge, S. Y. Tan, X. H. Niu *et al.*, Observation of possible topological in-gap surface states in the Kondo insulator SmB_6 by photoemission, Nat. Commun. **4**, 3010 (2010).

[8] W. Liu, J. Zhao, F. Meng, A. Rahman, Y. Qin, J. Fan, L. Pi, Z. Tian, H. Du, L. Zhang, and Y. Zhang, Critical behavior of the magnetic Weyl semimetal PrAlGe, Phys. Rev. B **103**, 214401 (2021).

[9] H.-Y. Yang, B. Singh, J. Gaudet, B. Lu, C.-Y. Huang, W.-C. Chiu, S.-M. Huang, B. Wang, F. Bahrami, B. Xu *et al.*, Noncollinear ferromagnetic Weyl semimetal with anisotropic anomalous Hall effect, Phys. Rev. B **103**, 115143 (2021).

[10] M. A. Ruderman and C. Kittel, Indirect exchange coupling of nuclear magnetic moments by conduction electrons, Phys. Rev. **96**, 99 (1954).

[11] K. Yosida, Magnetic properties of Cu-Mn alloys, Phys. Rev. **106**, 893 (1957).

[12] G. R. Stewart, Heavy-fermion systems, Rev. Mod. Phys. **56**, 755 (1984).

[13] S. Doniach, The Kondo lattice and weak antiferromagnetism, Physica B+C **91**, 231 (1977).

[14] A. J. Schofield, Non-Fermi liquids, Contemp. Phys. **40**, 95 (1999).

[15] G. R. Stewart, Non-Fermi-liquid behavior in d- and f-electron metals, Rev. Mod. Phys. **73**, 797 (2001).

[16] Q. Si, Quantum criticality and global phase diagram of magnetic heavy fermions, Phys. Stat. Sol. B **247**, 476 (2010).

[17] J. A. Hertz, Quantum critical phenomena, Phys. Rev. B **14**, 1165 (1976).

[18] A. J. Millis, Effect of a nonzero temperature on quantum critical points in itinerant fermion systems, Phys. Rev. B **48**, 7183 (1993).

[19] M. Vojta, From itinerant to local-moment antiferromagnetism in Kondo lattices: Adiabatic continuity versus quantum phase transitions, Phys. Rev. B **78**, 125109 (2008).

[20] Y. Tokiwa, C. Stingl, M.-S. Kim, T. Takabatake, and P. Gegenwart, Characteristic signatures of quantum criticality driven by geometrical frustration, Sci. Adv. **1**, e1500001 (2015).

[21] S. Nakatsuji, Y. Machida, Y. Maeno, T. Tayama, T. Sakakibara, J. van Duijn, L. Balicas, J. N. Millican, R. T. Macaluso, and J. Y. Chan, Metallic spin-liquid behavior of the geometrically frustrated Kondo lattice $Pr_2Ir_2O_7$, Phys. Rev. Lett. **96**, 087204 (2006).

[22] R. Tripathi, D. T. Adroja, C. Ritter, S. Sharma, C. Yang, A. D. Hillier, M. M. Koza, F. Demmel, A. Sundaresan, S. Langridge *et al.*, Quantum critical spin-liquid-like behavior in the $S = 1/2$ quasi-kagome lattice compound $CeRh_{1-x}Pd_xSn$ investigated using muon spin relaxation and neutron scattering, Phys. Rev. B **106**, 064436 (2022).

[23] Y. Shimura, A. Wörl, M. Sundermann, S. Tsuda, D. T. Adroja, A. Bhattacharyya, A. M. Strydom, A. D. Hillier, F. L. Pratt, A. Gloskovskii *et al.*, Antiferromagnetic correlations in strongly valence fluctuating CeIrSn, Phys. Rev. Lett. **126**, 217202 (2021).

[24] T. Okubo, S. Chung, and H. Kawamura, Multiple-q states and the skyrmion lattice of the triangular-lattice Heisenberg antiferromagnet under magnetic fields, Phys. Rev. Lett. **108**, 017206 (2012).

[25] A. O. Leonov and M. Mostovoy, Multiply periodic states and isolated skyrmions in an anisotropic frustrated magnet, Nat. Commun. **6**, 8275 (2015).

[26] V. Fritsch, C.-L. Huang, N. Bagrets, K. Grube, S. Schumann, and H. v. Löhneysen, Magnetization and specific heat of $CePd_{1-x}Ni_xAl$, Phys. Status Solidi B **250**, 506 (2013).

[27] M. Majumder, R. Gupta, H. Luetkens, R. Khasanov, O. Stockert, P. Gegenwart, and V. Fritsch, Spin-liquid signatures in the quantum critical regime of pressurized CePdAl, Phys. Rev. B **105**, L180402 (2022).

[28] H. Zhao, J. Zhang, M. Lyu, S. Bachus, Y. Tokiwa, P. Gegenwart, S. Zhang, J. Cheng, Y.-f. Yang, G. Chen *et al.*, Quantum-critical phase from frustrated magnetism in a strongly correlated metal, Nat. Phys. **15**, 1261 (2019).

[29] Z. Huesges, S. Lucas, S. Wunderlich, F. Yokaichiya, K. Prokeš, K. Schmalzl, M.-H. Lemée-Cailleau, B. Pedersen, V. Fritsch, H. v. Löhneysen *et al.*, Evolution of the partially frustrated magnetic order in $CePd_{1-x}Ni_xAl$, Phys. Rev. B **96**, 144405 (2017).

[30] E. M. Kenney, C. U. Segre, W. Lafargue-Dit-Hauret, O. I. Lebedev, M. Abramchuk, A. Berlie, S. P. Cottrell, G. Simutis, F. Bahrami, N. E. Mordvinova *et al.*, Coexistence of static and dynamic magnetism in the Kitaev spin liquid material Cu_2IrO_3, Phys. Rev. B **100**, 094418 (2019).

[31] A. A. Kulbakov, R. Sarkar, O. Janson, S. Dengre, T. Weinhold, E. M. Moshkina, P. Y. Portnichenko, H. Luetkens, F. Yokaichiya, A. S. Sukhanov *et al.*, Destruction of long-range magnetic order in an external magnetic field and the associated spin dynamics in Cu_2GaBO_5 and Cu_2AlBO_5 ludwigites, Phys. Rev. B **103**, 024447 (2021).

[32] K. Horigane, M. Fujii, H. Okabe, K. Kobayashi, R. Horie, H. Ishii, Y. F. Liao, Y. Kubozono, A. Koda, R. Kadono *et al.*, Magnetic phase diagram of $Sr_{2-x}La_xIrO_4$ synthesized by mechanical alloying, Phys. Rev. B **97**, 064425 (2018).

[33] R. Dally, T. Hogan, A. Amato, H. Luetkens, C. Baines, J. Rodriguez-Rivera, M. J. Graf, and S. D. Wilson, Short-range correlations in the magnetic ground state of $Na_4Ir_3O_8$, Phys. Rev. Lett. **113**, 247601 (2014).

[34] I. Yamauchi, K. Nawa, M. Hiraishi, M. Miyazaki, A. Koda, K. M. Kojima, R. Kadono, H. Nakao, R. Kumai, Y. Murakami *et al.*, Structural anomalies and short-range magnetic correlations in the orbitally degenerate system Sr_2VO_4, Phys. Rev. B **92**, 064408 (2015).

[35] A. M. Hallas, J. Gaudet, M. N. Wilson, T. J. Munsie, A. A. Aczel, M. B. Stone, R. S. Freitas, A. M. Arevalo-Lopez, J. P. Attfield, M. Tachibana *et al.*, XY antiferromagnetic ground state in the effective $S = \frac{1}{2}$ pyrochlore $Yb_2Ge_2O_7$, Phys. Rev. B **93**, 104405 (2016).

[36] S.-H. Do, W.-J. Lee, S. Lee, Y. S. Choi, K.-J. Lee, D. I. Gorbunov, J. Wosnitza, B. J. Suh, and K.-Y. Choi, Short-range quasistatic order and critical spin correlations in α-$Ru_{1-x}Ir_xCl_3$, Phys. Rev. B **98**, 014407 (2018).

[37] R. Wang, A. Gebretsadik, S. Ubaid-Kassis, A. Schroeder, T. Vojta, P. J. Baker, F. L. Pratt, S. J. Blundell, T. Lancaster, I. Franke *et al.*, Quantum Griffiths phase inside the ferromagnetic phase of $Ni_{1-x}V_x$, Phys. Rev. Lett. **118**, 267202 (2017).

[38] Z. Zhang, J. Li, M. Xie, W. Zhuo, D. T. Adroja, P. J. Baker, T. G. Perring, A. Zhang, F. Jin, J. Ji *et al.*, Low-energy spin dynamics of the quantum spin liquid candidate $NaYbSe_2$, Phys. Rev. B **106**, 085115 (2022).

[39] Y. Li, D. Adroja, P. K. Biswas, P. J. Baker, Q. Zhang, J. Liu, A. A. Tsirlin, P. Gegenwart, and Q. Zhang, Muon spin relaxation evidence for the $U(1)$ quantum spin-liquid ground state in the triangular antiferromagnet $YbMgGaO_4$, Phys. Rev. Lett. **117**, 097201 (2016).

[40] M. R. Cantarino, R. P. Amaral, R. S. Freitas, J. C. R. Araújo, R. Lora-Serrano, H. Luetkens, C. Baines, S. Bräuninger, V. Grinenko, R. Sarkar *et al.*, Dynamic magnetism in the disordered hexagonal double perovskite $BaTi_{1/2}Mn_{1/2}O_3$, Phys. Rev. B **99**, 054412 (2019).

[41] M. Baenitz, P. Schlender, J. Sichelschmidt, Y. A. Onykiienko, Z. Zangeneh, K. M. Ranjith, R. Sarkar, L. Hozoi, H. C. Walker, J. C. Orain *et al.*, $NaYbS_2$: A planar spin-$\frac{1}{2}$ triangular-lattice magnet and putative spin liquid, Phys. Rev. B **98**, 220409(R) (2018).

[42] S. Kundu, A. Shahee, A. Chakraborty, K. M. Ranjith, B. Koo, J. Sichelschmidt, M. T. F. Telling, P. K. Biswas, M. Baenitz, I. Dasgupta *et al.*, Gapless quantum spin liquid in the triangular system $Sr_3CuSb_2O_9$, Phys. Rev. Lett. **125**, 267202 (2020).

[43] Q. Chen, R. Sinclair, A. Akbari-Sharbaf, Q. Huang, Z. Dun, E. S. Choi, M. Mourigal, A. Verrier, R. Rouane, X. Bazier-Matte *et al.*, Magnetic order and spin liquid behavior in $[Mo_3]^{11+}$ molecular magnets, Phys. Rev. Mater. **6**, 044414 (2022).

[44] J. C. Orain, L. Clark, F. Bert, P. Mendels, P. Attfield, F. H. Aidoudi, R. E. Morris, P. Lightfoot, A. Amato, and C. Baines, μSR study of a quantum spin liquid candidate: the $S = \frac{1}{2}$ vanadium oxyfluoride kagome antiferromagnet, J. Phys.: Conf. Ser. **551**, 012004 (2014).

[45] Y. J. Uemura, T. Yamazaki, D. R. Harshman, M. Senba, and E. J. Ansaldo, Muon-spin relaxation in AuFe and CuMn spin glasses, Phys. Rev. B **31**, 546 (1985).

[46] D. E. MacLaughlin, O. O. Bernal, R. H. Heffner, G. J. Nieuwenhuys, M. S. Rose, J. E. Sonier, B. Andraka, R. Chau, and M. B. Maple, Glassy spin dynamics in non-Fermi-liquid $UCu_{5-x}Pd_x$, $x = 1.0$ and 1.5, Phys. Rev. Lett. **87**, 066402 (2001).

[47] D. E. MacLaughlin, R. H. Heffner, O. O. Bernal, K. Ishida, J. E. Sonier, G. J. Nieuwenhuys, M. B. Maple, and G. R. Stewart, Disorder, inhomogeneity and spin dynamics in f-electron non-Fermi liquid systems, J. Phys.: Condens. Matter **16**, S4479 (2004).

[48] D. T. Adroja, A. D. Hillier, J.-G. Park, W. Kockelmann, K. A. McEwen, B. D. Rainford, K.-H. Jang, C. Geibel, and T. Takabatake, Muon spin relaxation study of non-Fermi-liquid behavior near the ferromagnetic quantum critical point in $CePd_{0.15}Rh_{0.85}$, Phys. Rev. B **78**, 014412 (2008).

[49] R. Tripathi, D. Das, P. K. Biswas, D. T. Adroja, A. D. Hillier, and Z. Hossain, Quantum Griffiths phase near an antiferromagnetic quantum critical point: Muon spin relaxation study of $Ce(Cu_{1-x}Co_x)_2Ge_2$, Phys. Rev. B **99**, 224424 (2019).

[50] O. O. Bernal, D. E. MacLaughlin, H. G. Lukefahr, and B. Andraka, Dynamics in canonical spin glasses observed by muon spin depolarization, Phys. Rev. Lett. **75**, 2023 (1995).

[51] M. C. de Andrade, R. Chau, R. P. Dickey, N. R. Dilley, E. J. Freeman, D. A. Gajewski, M. B. Maple, R. Movshovich, A. H. Castro Neto, G. Castilla *et al.*, Evidence for a common physical description of non-Fermi-liquid behavior in chemically substituted f-electron systems, Phys. Rev. Lett. **81**, 5620 (1998).

[52] S. Vishvakarma and V. Srinivas, Non-Fermi liquid behavior and signature of Griffiths phase in Ni-Cr binary alloy, J. Appl. Phys. **129**, 143901 (2021).

[53] V. V. Krishnamurthy, K. Nagamine, I. Watanabe, K. Nishiyama, S. Ohira, M. Ishikawa, D. H. Eom, T. Ishikawa, and T. M. Briere Non-Fermi-liquid spin dynamics in $CeCoGe_{3-x}Si_x$ for $x = 1.2$ and 1.5, Phys. Rev. Lett. **88**, 046402 (2002).

[54] A. Keren, P. Mendels, I. A. Campbell, and J. Lord, Probing the spin-spin dynamical autocorrelation function in a spin glass above T_g via muon spin relaxation, Phys. Rev. Lett. **77**, 1386 (1996).

[55] I. A. Campbell, A. Amato, F. N. Gygax, D. Herlach, A. Schenck, R. Cywinski, and S. H. Kilcoyne, Dynamics in canonical spin glasses observed by muon spin depolarization, Phys. Rev. Lett. **72**, 1291 (1994).

[56] V. Fritsch, N. Bagrets, G. Goll, W. Kittler, M. J. Wolf, K. Grube, C.-L. Huang, and H. v. Löhneysen, Approaching quantum criticality in a partially geometrically frustrated heavy-fermion metal, Phys. Rev. B **89**, 054416 (2014).